Transmembrane Segment Packing of the Na+/Ca2+ Exchanger Investigated with Chemical Cross-Linkers

ARTICLE *in* BIOCHEMISTRY · OCTOBER 2010

Impact Factor: 3.02 · DOI: 10.1021/bi101173c · Source: PubMed

5 AUTHORS, INCLUDING:

Xiaoyan Ren
University of California, Los Angeles
24 PUBLICATIONS **165** CITATIONS
SEE PROFILE

Zhilin Qu
University of California, Los Angeles
201 PUBLICATIONS **6,629** CITATIONS
SEE PROFILE

Published in final edited form as:
Biochemistry. 2010 October 5; 49(39): 8585–8591. doi:10.1021/bi101173c.

TRANSMEMBRANE SEGMENT PACKING OF THE Na^+/Ca^{2+} EXCHANGER INVESTIGATED WITH CHEMICAL CROSSLINKERS

Xiaoyan Ren, **Debora A. Nicoll**, **Lida Xu**, **Zhilin Qu**, and **Kenneth D. Philipson***
Departments of Physiology and Medicine and the Cardiovascular Research Laboratories, David Geffen School of Medicine at UCLA, Los Angeles, California 90095-1760

Abstract

The Na^+/Ca^{2+} exchanger (NCX1) is a plasma membrane protein important in regulating Ca^{2+} in cardiac myocytes. The topological model is comprised of nine transmembrane segments (TMSs). To gain insights into the TMS packing arrangement of NCX1, we performed cysteine crosslinking experiments. Pairs of amino acids in different TMSs were mutated to cysteine on the backbone of a cysteineless NCX1. The mutated exchangers were expressed in an insect cell line and treated with cysteine-specific chemical crosslinkers followed by SDS-PAGE to determine the proximity of the introduced cysteines. Previously we showed that TMSs 2, 3, 7, and 8 are near one another and that residues in TMSs 1 and 2 are close to TMS 6. In this report, we use the same approach to provide evidence for the arrangement of the remaining three TMSs (4, 5, and 9). We present a computer-generated 2-dimensional model of transmembrane packing that minimizes the lengths of all crosslinks.

The cardiac Na^+/Ca^{2+} exchanger (NCX1) is an integral membrane protein that extrudes Ca^{2+} from myocardial cells by using the energy of the Na^+ gradient. The exchanger is important in maintaining the balance of Ca^{2+} during cardiac excitation-contraction coupling. Abnormal expression of NCX1 is associated with cardiac malfunction and NCX1 is a potential therapeutic target for regulation of cardiac function and treatment of disease (1,2).

In the current topological model (Fig. 1), NCX1 is composed of nine transmembrane segments (TMSs) organized in an amino-terminal cluster of 5 TMSs (N-Cluster) and a carboxyl-terminal cluster of 4 TMSs (C-Cluster) connected by a large intracellular loop containing two regulatory Ca^{2+} binding domains (CBD1 and CBD2) (3–5). The structures of CBD1 and CBD2 have been resolved and the key residues for binding regulatory Ca^{2+} are known (6–8). In contrast, there has been no direct identification of TMS residues that are critical for the binding of transported Ca^{2+} or Na^+ although mutations to some residues can alter Na^+ (4,5,9) or Ca^{2+} (4) affinity. To obtain more information about substrate binding and translocation by NCX1, the best approach is to resolve the three-dimensional structure of the full-length protein. This structure, however, remains elusive.

An alternative method for obtaining structural information is the use of disulfide crosslinking to identify residues that are in close proximity (10). Santacruz-Toloza et al. (11) first noted that a disulfide bond between a residue in the N-cluster with a residue in the C-cluster of NCX1 causes a shift in mobility on SDS-PAGE under non-reducing conditions. Qiu and colleagues (12) took advantage of that observation and introduced pairs of cysteines

*Corresponding author. Department of Physiology, UCLA, 675 Charles E. Young Dr. S., MRL 3-645, Los Angeles CA 90095-1760. Tel: 310-825-7679. Fax: 310-206-7777. KPhilipson@mednet.ucla.edu..

Supporting Information Available Detailed methods and additional crosslinking data. This material is available free of charge via the Internet at http://pubs.acs.org.

into NCX1 to identify disulfide-induced mobility shifts. They examined the arrangement of TMSs 2, 3, 7 and 8 of NCX1 and found that TMS 7 is close to TMS 3 near the intracellular side of the membrane and is in the vicinity of TMS 2 near the extracellular surface. Also, TMS 2 must adjoin TMS 8. This showed that two functionally important domains in NCX1, the α-1 and α-2 repeats (13), are close to each other.

Later, Ren and colleagues (14) showed that residues in TMSs 1 and 2 are close to cysteine 768 in TMS 6. Cysteine 768 crosslinked with residues at both ends of TMSs 1 and 2 and is likely located towards the middle of TMS 6. Additionally, NCX1 can form dimers as also identified by crosslinking approaches (15). Dimerization occurs along a face of the protein that includes parts of TMS 1 and TMS 2.

In this work, we concentrate on TMSs 4, 5, and 9 and how these TMSs are arranged with respect to the other TMSs. Based on all the disulfide crosslinking data, we propose a two-dimensional arrangement for the nine TMSs of NCX1 based on computer modeling.

EXPERIMENTAL PROCEDURES

Construction of exchanger cysteine mutants

Single cysteine mutants were prepared by the Quick Change site-directed mutagenesis method (Agilent Technologies) (3). Mutations were generated in 300–500 base pair cassettes and verified by sequencing. Full-length exchangers with single or double mutations were constructed by subcloning the mutated cassettes into the cysteineless exchanger.

Expression of the NCX1 cysteine mutants in Insect High Five cells

A lepidopteran insect cell expression system BTI-TN-5B1-4 (High Five, Invitrogen) was used for transient transfection of NCX1 cysteine mutants. High Five cells were cultured at 27° in Express Five SFM (Invitrogen) supplemented with 20 mM glutamine and 1% penicillin-streptomycin.

Mutant NCX1 cDNAs were subcloned into the pIE1/153A (V4-) triple expression vector (Cytostore) and High Five insect cells were transfected using Cellfectin reagent (Invitrogen). 24 h post-transfection, Na^+ gradient-dependent $^{45}Ca^{2+}$ uptake into the High Five cells was measured (12). Cells were harvested and washed twice with washing buffer (10 mM MOPS, pH 7.4, 140 mM NaCl) and then loaded with Na^+ by incubation with washing buffer containing 1 mM $MgCl_2$, 0.4 mM ouabain and 25 μM nystatin for 10 min at room temperature. Nystatin was removed from the cells by two washes with washing buffer plus 0.4 mM ouabain. Uptake was initiated by resuspending the cell pellet in assay medium: 10 mM MOPS, pH 7.4, 140 mM KCl (or NaCl as control), 25 μM $CaCl_2$, 0.4 mM ouabain, and 5 μCi/ml $^{45}Ca^{2+}$. After 10 min, the reaction was stopped by adding 1 ml of ice-cold quenching solution (140 mM KCl, 1 mM EGTA) followed by two additional washes with quenching solution. Cell pellets were dissolved in 1N NaOH at 60 °C for 30 min. Aliquots of samples were subjected to scintillation counting and protein assay (Micro BCA, Pierce).

Crosslinking in intact cells

Intact cells were rinsed with washing buffer and crosslinking was carried out at room temperature by addition of oxidative reagent (CuPhe), thiol-specific homobifunctional crosslinker (*p*-PDM), maleimide crosslinker BM(PEG)2 (Pierce) or MTS crosslinkers (Toronto Research Chemicals) to the intact cell suspension. The final concentrations of reagents were 1 mM $CuSO_4$ and 3 mM phenanthroline, or 0.5 mM *p*-PDM or BM(PEG)2, or 0.5 mM MTS crosslinkers 2M, 3M, 6M, 8M, 11M, 14M or 17M. Some samples were pre-incubated with 10 mM NEM or MTSES. Reactions were terminated after 20 min by addition

of NEM (10 mM). Cells were lysed with 1% Triton X-100 plus protease inhibitors (complete, EDTA-free, Roche). Aliquots were subjected to 7.5% SDS-PAGE in the absence of reducing reagents and immunoblot analysis was carried out with NCX1 antibody R3F1(16). All experiments were performed at least three times and representative data are shown.

Membrane vesicle preparation, crosslinking, and vesicular $^{45}Ca^{2+}$ uptake

Transfected cells were washed twice with washing buffer, resuspended in washing buffer, and homogenized with 10 strokes in a Dounce homogenizer. After centrifugation at 100,000 × g for 30 min at 4°C, the pellet was resuspended in washing buffer. The sample was then passed through a 23-gauge needle 20 times and centrifuged for 5 min at 1258 × g at 4°C to remove cell debris and nuclei. The supernatant was centrifuged at 100,000 × g for 30 min at 4°C to collect the crude membrane pellet which was resuspended in washing buffer. Crosslinking was induced by the addition of 50 μM of 3M or 17M at room temperature for 30 min. Aliquots of the control or crosslinked membrane vesicles were run on SDS PAGE. Separate aliquots of vesicles were used for $^{45}Ca^{2+}$ uptake. Na^{+}-dependent Ca^{2+} uptake into vesicles was measured as previously described in detail (17). Crosslinked membrane vesicles (5 μl) were washed twice with washing buffer and rapidly diluted into 0.25 ml of uptake medium containing 140 mM KCl (or NaCl for blanks), 0.3 mCi $^{45}Ca^{2+}$, 10 μM Ca^{2+}, 0.4 mM valinomycin, 10 mM MOPS, pH 7.4 at 37°C. The uptake reaction was stopped at 3 s with 30 μl of 140 mM KCl and 10 mM EGTA, immediately followed by addition of 1 ml ice cold 140 mM KCl, 1 mM EGTA. The vesicles were collected by filtration and washed twice with ice cold 140 mM KCl, 1 mM EGTA. All experiments were performed in duplicate, with an n of 5 to 11. Data are expressed as means ± SD.

Modeling helix packing

Each TMS was reduced to its helical wheel projection of a circle with consecutive amino acids separated by 100° along the circumference of the circle. The nine circles (12 units in diameter) were then rotated and packed into a square of 60 units on a side such as to minimize the total area of the circles that are cut by the crosslinks between residues. We included the constraint that TMSs 4 and 5 must be adjacent (due to the short linker between the two). The resulting arrangement of TMSs was then adjusted to minimize the sum of the lengths of the crosslinks. For more detail, see “Supplemental Information”.

Hazardous Procedures

All procedures involving the use of $^{45}Ca^{2+}$ were performed under the guidance and following the rules of the Radiation Safety Office at UCLA.

RESULTS

Activity of paired cysteine mutants of NCX1

Single cysteines were first introduced into a cysteineless NCX1 mutant (12). NCX1 mutants with two cysteines were then constructed by subcloning and were expressed in insect High Five cells using the pIE1/153A (V4-) triple expression vector. The expression level (both activity and immunoreactive protein) of NCX1 cysteine mutants expressed with this vector was about 50% higher than when expressed with the pIB/V5-His vector used in our previous work (14) (data not shown). Only mutants having at least 20% of WT NCX1 activity (Table S1) were selected for crosslinking experiments. The experiments focus on TMSs 4, 5, and 9 (Fig. 1) since other TMSs have been investigated previously (12,14).

Crosslinkers

We used three different types of crosslinkers. CuPhe is an oxidative reagent, which can catalyze disulfide formation between sulfhydryl groups. The resultant disulfide bond is about 2 Å in length. *p*-PDM and BM(PEG)2 are dimaleimide sulfhydryl crosslinkers that cannot be cleaved by reducing agents. *p*-PDM is a rigid crosslinker with a linker distance of 12 Å and has been used with NCX1 previously (12,14). BM(PEG)2 is more flexible and has a linker distance of 15 Å. MTS crosslinkers react selectively with cysteines, resulting in a disulfide attachment of the spacer group. The MTS reagents we chose are flexible crosslinkers (18) including 2M (4 Å), 3M (5 Å), 6M (9 Å), 8M (11 Å), 11M (14 Å), 14M (16 Å) and 17M (21 Å). The appoximate spacer lengths deviate by 1 to 2 Å (19). In control experiments using the mutant S188C/T877C and the crosslinkers 2M, 8M, and 14M at 0.5 mM at room temperature, we found that a 20 min exposure was sufficient to maximize crosslinking (Supplemental Fig. S4). All the crosslinkers chosen for this study are membrane permeable and crosslinking experiments were carried out using intact cells unless otherwise specified.

Crosslinking between residues in TMS 4 and the C-cluster of NCX1

TMS 4 to TMS 6—Residue 188, modeled to be close to the extracellular side of TMS 4, was paired with residue 767 or 768 in TMS 6. Both S188C/A767C (not shown) and S188C/A768C mutants display wild-type levels of activity (Suppl. Table S1) but no crosslinking (Fig. 2A). Thus, proximity of TMSs 4 and 6 was not detected.

TMS 4 to TMS 7—In previous work (12), residues modeled to be near the intracellular sides of TMSs 4 and 7 did not form crosslinks. 12 pairs of cysteine mutants were constructed between TMS 4 and 7, four of which were active. All four pairs showed mobility shifts upon application of crosslinkers (Fig. 2B). Mutants T181C/V804C and T181C/V806C can be crosslinked with thiol reagents 2–9 Å in length but not with the longer bimaleimide crosslinking reagents. S188C/V804C and S188C/V806C could be crosslinked with a greater array of crosslinkers with mobility shifts observed when using crosslinkers with spacer arms between 2 and 15 Å (Fig. 2B) or longer (14M and 17M, data not shown). For both mutants containing S188C, crosslinker-induced mobility shifts could be inhibited by pre-incubation with NEM. On a helical wheel projection of TMS 4 (see Fig. 6), residues 181 and 188 are within 20° of each other. In TMS 7, residues 804 and 806 are separated by 160°. These residues are modeled to be near the extracellular surface (Fig. 1).

TMS 4 to TMS 8—We paired a cysteine at position 188 (near the extracellular surface) with cysteines at 892 (at the extracellular side) or 877 (towards the intracellular side) in TMS 8. We expected that crosslinking would be more likely to be detected with mutant S188C/Y892C than with S188C/T877C. However, we obtained an unexpected result. Crosslinking was observed in mutant S188C/T877C (Fig. 2C) with crosslinkers ranging from 2 to 22 Å in length. Crosslinking was unaffected by the presence or absence of Na^+ in the extracellular medium (Supp. Fig. S5). No crosslinking was observed with mutant S188C/Y892C (Fig. 2C, lower panel).

TMS 4 to TMS 9—Proximity between TMSs 4 and 9 was not observed in previous work utilizing cysteines at positions 909 and 926 towards the ends of TMS 9 (12). Thus, we used residues modeled to be more towards the middle of TMS 9. Four mutants were constructed: T181C/S914C, T181C/L915C, S188C/S914C and S188C/L915C. All were active and all displayed crosslinking (Fig. 2D shows results for T181C/L915C and S188C/S914C) implying that TMSs 4 and 9 are in close proximity.

Crosslinking between residues in TMS 5 and the C-cluster of NCX1

Residue 210 in TMS 5 is a native cysteine. In a previous study, we combined C210 with cysteine residues in the C-cluster of NCX1 but were unable to detect crosslinking (12). We chose seven additional residues in TMSs 7, 8, and 9 to pair with residue 210. Of these seven pairs, five were active and four showed mobility shifts upon application of crosslinkers (Fig. 3). Crosslinking induced by 6M could be blocked by pre-incubation with NEM. The results show that TMS 5 is in proximity to TMS 7 and 9.

Crosslinking between residues in TMS 9 and the N-cluster of NCX1

Previously, residues in TMS 9 were paired with residues in TMSs 1–5 (12), but none of the active mutants could be crosslinked by CuPhe, *o*-PDM or *p*-PDM when expressed in HEK293 cells. However, inactive mutant 117/909 did display crosslinking. Thus, we subcloned S117C/K909C and another previously examined mutant, A122C/K909C, into the pIE1/153A (V4-) triple expression vector and expressed them in insect High Five cells (Table 1). No activity was detected with either mutant. We then tried pairing native cysteine 914 or L915C, in the middle of TMS 9, with residues in TMSs 2–5. The 12 mutants we examined all showed Na^+ gradient-dependent Ca^{2+} transport and were then treated with crosslinking reagents. We observed crosslinked product for 11 mutants as determined by decreased electrophoretic mobility. Fig. 4 shows results obtained with a negative mutant (A914C/S117C) and two positive mutants (L915C/A122C, L915C/A151C). Our results indicate that TMS 9 is in proximity with TMSs 2, 3, 4, and 5.

Is residue 877 in TMS 8 accessible to residues at the extracellular side of the membrane?

Based on a combination of hydropathy analysis, cysteine mutagenesis followed by sulfhydryl modification, immunolocalization, and functional measurements, the exchanger is modeled to have nine transmembrane segments and two re-entrant loops (3–5) (Fig. 1). TMS 8 is modeled to contain 20 amino acids beginning with the intracellular L872 to the extracellular Y892. Thus, residue 877 is modeled to be near the intracellular side of the membrane. That model is supported by results that show nearby residue 875 is accessible to intracellular but not extracellular application of MTSEA (3). On the other hand, we observe crosslinking between T877C and S188C (Fig. 2C). We did further experiments to confirm the extracellular accessibility of residue 877.

In the wild-type NCX1, residues 20 and 122 are cysteines. C20 is in the amino terminal loop which is glycosylated (20) and clearly extracellular. In the native exchanger, C20 forms a disulfide bond with C792 in the loop between TMS 6 and 7 which therefore is also extracellular (11). C122 is at the extracellular surface of TMS 2. Residue 188 is modeled to be in TMS 4 near the extracellular surface. To confirm that residue 188 is near the outside of the membrane, we paired it with C792. Mutant S188C/A792C showed good crosslinking with 17M (Fig. 5A). Treatment with 17M resulted in crosslinking between cysteine 877 and the extracellular cysteines at positions 20, 122, and 188. The relative extents of crosslinking were A20C<A122C<S188C (Fig. 5A, B). Pre-incubation with the membrane impermeable MTS reagent MTSES or membrane permeable agent NEM completely blocked crosslinking (Fig. 5A). Residue 877 is indeed accessible to the extracellular surface of the membrane.

We also examined the effects of crosslinking on the activity of mutants A20C/T877C, A122C/T877C and S188C/T877C. In preliminary experiments, we found nospecific inhibition of cysless NCX activity in High Five cells by crosslinking agents (not shown). Therefore, for these experiments, crosslinking and exchanger activity were measured in membrane vesicles prepared from High Five cells. Gels of crosslinked samples using membrane vesicles were similar to those obtained using intact cells (Suppl. Fig. S6). To check if exchanger activity was affected by crosslinking, we first tested the effect of

crosslinkers on the activity of the cysteineless exchanger. The crosslinkers 3M and 17M at 50 μM had no significant effect (Fig. 5C). With crosslinker 3M, the A20C/T877C exchanger showed no crosslinking (Fig. 5B) and no effect on activity (Fig. 5C) but 17M crosslinked residues 20C and 877C and stimulated NCX1 activity. For mutant A122C/T877C, 3M and 17M both caused significant crosslinking and inhibition of activity although only the inhibition by 17M was significant (Fig. 5C). For mutant S188C/T877C a large fraction of the protein was crosslinked by 3M or 17 M (Fig. 5B) and both crosslinkers significantly inhibited NCX1 activity. The results suggest that restraining the movements between residues with crosslinkers have modest effects on ion transport. Alternatively, direct modification of the introduced cysteine may be the cause of inhibition and we cannot eliminate this possibility.

Helix packing of NCX1 predicted by computer modeling

Based on all crosslinking data to date (summarized in Table 1), a helix-packing model for NCX1 was obtained by computer modeling with the following constraints. First, we minimized the sum of the distance between crosslinked residues. Second, we minimized lines connecting crosslinked residues that bisected TMSs. Third, TMS 4 and TMS 5 are constrained to be adjacent because there are only 3 amino acids between them. The resulting model is shown in Fig.6 and Supplemental Fig S6 shows the locations of crosslinks with an axis perpendicular to the membrane surface. When the pairs of residues that did not form crosslinks are mapped on to this model (Suppl. Fig. S7) connecting lines frequently cross through TMSs.

DISCUSSION

We have used a combination of cysteine substitution mutagenesis followed by disulfide crosslinking to gain insights into the helix-packing structure of the TMSs of NCX1. With the results presented here, in combination with two earlier studies, we have observed crosslinking between each of the TMSs of the N-cluster to at least two TMSs in the C-cluster of NCX1 (and vice versa) and are able to present the packing model for NCX1 shown in Fig. 6. At best, this arrangement is a 2-dimensional slice through the protein.

To obtain our helix-packing model, we use two assumptions: first, that the TMSs are all perpendicular to the membrane and, second, that the TMSs are all continuous α-helices. Neither assumption is likely to be fully accurate. With the growing number of crystal structures of membrane proteins, it is clear that most membrane proteins have TMSs that cross the membrane at an angle. Also, discontinuities in the α-helices are a common theme, and several transporters have non-α-helical portions of TMSs that are important participants in interactions with substrates (21). Prolines in α-helices are one source of discontinuities (22), but discontinuities may also occur for other reasons. There are prolines present in TMSs 2 (P112), 5 (P208), and 7 (P813). TMSs 2 and 7 also have a conserved GXXXP motif which places a glycine and proline one helical turn apart perhaps giving these TMSs considerable flexibility (23). With a proline-induced discontinuity, the crosslinked residues 101 and 102 may not be in a strict helical wheel alignment with respect to residues 117 and 122 in TMS 2 as shown in Fig. 6. The same would be true for residues 804 and 806 with respect to residues 815 and 821 of TMS 7.

While the crosslinking studies have by no means been exhaustive, it appears that the most `packable' of the TMSs are TMS 2 and TMS 7, both segments of the α-repeats (Fig. 1). The α-repeats are regions of sequence similarity that are the apparent result of a gene duplication event. There is much evidence that the α-repeats are critical in the NCX1 transport process. For TMSs 2 and 7 we have observed at least one crosslink with each TMS of the opposite TMS cluster. The packability of TMSs 2 and 7 is predicted by calculating the helix-packing

moment for each TMS of NCX1. Helix-packing moments help identify the packing interfaces in membrane proteins containing multiple transmembrane helices (24). In NCX1, TMSs 2 and 7 have 15 and 11 residues with significant packing moments, respectively. No other TMS has more than 6 residues with significant packing moments. Thus, our observations and the prediction agree that TMSs 2 and 7 interact with multiple TMSs and are likely to have fewer interactions with the bilayer.

A number of residues in TMSs 2, 3, 5 and 7 have been implicated in the ion exchange process of NCX1. Mutations of these residues result in transporters that show no Na^+/Ca^{2+} exchange activity or exchangers with altered ion selectivity/apparent affinities. When mapped onto the TMS helical wheels in our model (grey arcs in Fig. 6), these residues are all on interior facing portions of the TMSs. For TMS 2, the helical wheel surface contains three residues (S109, S110, E113) (13) that when mutated result in `dead' exchangers and one residue (T103) (5) whose mutation results in altered Na^+ affinity and selectivity. In TMS 3, mutants at residues 139, 140, 143, and 147 either have no activity or significantly reduced apparent affinities for Na^+ (9). In the helical wheel projection, these residues are all adjacent to C151, which is capable of crosslinking with TMSs 7–9. TMS 5 shares a small amount of sequence similarity to the Na^+-pump and mutants E199Q and T203V are inactive (13). Those residues are on either side of C210, which can form crosslinks with TMSs 7 and 9. Mutations in TMS 7 that result in no Ca^{2+} transport activity are to residues T810, S811, D814 and S818 (13). All of these residues map to the same side of the TMS 7 helical wheel defined by crosslinked residues 804 through 821. For TMSs 2 and 7, the arcs that define the regions of residues sensitive to mutagenesis are adjacent to the GXXXP motif. Thus, these functionally important regions may have increased flexibility. In sum, the helix-packing model is independently consistent with mutational analysis in positioning functionally important residues towards the interior of the protein.

The technique we used to determine which residues could form crosslinks took advantage of an earlier observation that crosslinks between the two clusters of TMSs result in a shift in mobility on SDS-PAGE. This limits the search for proximate residues to interactions between the two TMS clusters and we are unable to define interactions between TMSs within a cluster. From our helix-packing model, which was generated by minimizing the bisection of helical wheels by crosslinks and the sum of the lengths of the crosslinks, it appears that there is segregation of the two TMS clusters. The N-cluster is on one side of NCX1 and, with the exception of TMS 6, the C-cluster is on the other side. With that segregation and the inverted topology of the α-repeats, we anticipate that the 3-dimensional structure of NCX1 will fit into the growing list of membrane proteins whose TMSs are arranged with a 2-fold symmetry axis perpendicular to the plane of the membrane (18).

Especially notable is the accessibility of residue 877. We have previously shown in cysteine-modification experiments, that nearby residue 875 is in contact with the cytoplasm (3). Here, we show that residue 877 can form crosslinks with residues at the extracellular surface over a wide range of crosslinker lengths. This raises some interesting questions regarding the conformation of the NCX1 peptide in this region and/or the conformational changes that can occur here. We propose that residue 877 of TMS 8 is in a region of high flexibility or mobility that permits accessibility to extracellular crosslinking reagents. Perhaps this region is involved in forming the `rocker switch' (18) to allow alternating access of Na^+ and Ca^{2+} to either side of the membrane.

All pairs of residues that were used to generate the helix-packing model can be crosslinked with reagents having spacer arms that are 6.5 Å or smaller. Thus, our helix-packing model describes residues that come within at least 6.5 Å of one another. However, the fraction of time that any given pair of residues actually spend in close enough proximity to form

crosslinks may be quite small. Proteins are dynamic, not rigid, entities that exist in a continuum of conformational states with timescales that vary from fsec to sec (25,26). Since our crosslinking reactions were performed at room temperature for 20 min our results cannot describe a single snapshot of helix packing but rather a number of specific contacts that can occur with different conformations at a near physiologic temperature. We must await a crystal structure for NCX1 to obtain a single snapshot. With that in hand, our crosslinking data may provide insights into some of the movements NCX1 must undergo in a membrane compared to the static structure provided by crystals.

Supplementary Material

Refer to Web version on PubMed Central for supplementary material.

Acknowledgments

This work was supported by National Institutes of Health Grant HL-49101

Abbreviations and Footnotes

NCX1	Na^+/Ca^{2+} exchanger 1
TMS	transmembrane segment
PAGE	polyacrylamide gel electrophoresis
MTS	methanethiosulfonate
MOPS	4-morpholinepropanesulfonic acid
CuPhe	$CuSO_4$/phenanthroline
***o*-PDM**	*N*', *N*'- *o*-phenylenedimaleimide
***p*-PDM**	*N*', *N*'- *p*–phenylenedimaleimide
BM(PEG)2	1,8-bismaleimidodiethylene glycol
3M	1,3-propanediyl bismethanethiosulfonate
6M	1,6-hexanediyl bismethanethiosulfonate
8M	3,6-dioxaoctane-1,8-diyl bismethanethiosulfonate
11M	3,6,9-trioxaundecane-1,11-diyl-bismethanethiosulfonate
14M	3,6,9,12-tetraoxatetradecane-1,14-diyl-bismethanethiosulfonate
17M	3,6,9,12,15-pentaoxaheptadecane-1,17-diyl bismethanethiosulfonate
NEM	*N*-ethylmaleimide
MTSES	sodium (2-sulfonatoethyl) methanethiosulfonate
NEM	*N*-ethylmaleimide
WT	wild-type
HEK	human embryonic kidney

REFERENCES

(1). Philipson KD, Nicoll DA. Sodium-calcium exchange: a molecular perspective. Annu Rev Physiol. 2000; 62:111–133. [PubMed: 10845086]

(2). Blaustein MP, Lederer WJ. Sodium/calcium exchange: its physiological implications. Physiol Rev. 1999; 79:763–854. [PubMed: 10390518]

(3). Nicoll DA, Ottolia M, Lu L, Lu Y, Philipson KD. A new topological model of the cardiac sarcolemmal Na^+-Ca^{2+} exchanger. J Biol Chem. 1999; 274:910–917. [PubMed: 9873031]

(4). Iwamoto T, Uehara A, Imanaga I, Shigekawa M. The Na^+/Ca^{2+} exchanger NCX1 has oppositely oriented reentrant loop domains that contain conserved aspartic acids whose mutation alters its apparent Ca^{2+} affinity. J Biol Chem. 2000; 275:38571–38580. [PubMed: 10967097]

(5). Doering AE, Nicoll DA, Lu Y, Lu L, Weiss JN, Philipson KD. Topology of a functionally important region of the cardiac Na^+/Ca^{2+} exchanger. J Biol Chem. 1998; 273:778–783. [PubMed: 9422731]

(6). Nicoll DA, Sawaya MR, Kwon S, Cascio D, Philipson KD, Abramson J. The crystal structure of the primary Ca^{2+} sensor of the Na^+/Ca^{2+} exchanger reveals a novel Ca^{2+} binding motif. J Biol Chem. 2006; 281:21577–21581. [PubMed: 16774926]

(7). Hilge M, Aelen J, Vuister GW. Ca^{2+} regulation in the Na^+/Ca^{2+} exchanger involves two markedly different Ca^{2+} sensors. Mol Cell. 2006; 22:15–25. [PubMed: 16600866]

(8). Besserer GM, Ottolia M, Nicoll DA, Chaptal V, Cascio D, Philipson KD, Abramson J. The second Ca^{2+}-binding domain of the Na^+/Ca^{2+} exchanger is essential for regulation: crystal structures and mutational analysis. Proc Natl Acad Sci U S A. 2007; 104:18467–18472. [PubMed: 17962412]

(9). Ottolia M, Nicoll DA, Philipson KD. Mutational analysis of the alpha-1 repeat of the cardiac Na^+-Ca^{2+} exchanger. J Biol Chem. 2005; 280:1061–1069. [PubMed: 15519995]

(10). Falke JJ, Koshland DE Jr. Global flexibility in a sensory receptor: a site-directed cross-linking approach. Science. 1987; 237:1596–1600. [PubMed: 2820061]

(11). Santacruz-Toloza L, Ottolia M, Nicoll DA, Philipson KD. Functional analysis of a disulfide bond in the cardiac Na^+-Ca^{2+} exchanger. J Biol Chem. 2000; 275:182–188. [PubMed: 10617603]

(12). Qiu Z, Nicoll DA, Philipson KD. Helix packing of functionally important regions of the cardiac Na^+-Ca^{2+} exchanger. J Biol Chem. 2001; 276:194–199. [PubMed: 11035002]

(13). Nicoll DA, Hryshko LV, Matsuoka S, Frank JS, Philipson KD. Mutation of amino acid residues in the putative transmembrane segments of the cardiac sarcolemmal Na^+-Ca^{2+} exchanger. J Biol Chem. 1996; 271:13385–13391. [PubMed: 8662775]

(14). Ren X, Nicoll DA, Philipson KD. Helix packing of the cardiac Na^+-Ca^{2+} exchanger: proximity of transmembrane segments 1, 2, and 6. J Biol Chem. 2006; 281:22808–22814. [PubMed: 16785232]

(15). Ren X, Nicoll DA, Galang G, Philipson KD. Intermolecular cross-linking of Na^+-Ca^{2+} exchanger proteins: evidence for dimer formation. Biochemistry. 2008; 47:6081–6087. [PubMed: 18465877]

(16). Porzig H, Li Z, Nicoll DA, Philipson KD. Mapping of the cardiac sodium-calcium exchanger with monoclonal antibodies. Am J Physiol. 1993; 265:748–756.

(17). Vemuri R, Philipson KD. Phospholipid composition modulates the Na^+-Ca^{2+} exchange activity of cardiac sarcolemma in reconstituted vesicles. Biochim Biophys Acta. 1988; 937:258–268. [PubMed: 3276350]

(18). Zhou Y, Guan L, Freites JA, Kaback HR. Opening and closing of the periplasmic gate in lactose permease. Proc Natl Acad Sci U S A. 2008; 105:3774–3778. [PubMed: 18319336]

(19). Loo TW, Clarke DM. Determining the dimensions of the drug-binding domain of human P-glycoprotein using thiol cross-linking compounds as molecular rulers. J Biol Chem. 2001; 276:36877–36880. [PubMed: 11518701]

(20). Hryshko LV, Nicoll DA, Weiss JN, Philipson KD. Biosynthesis and initial processing of the cardiac sarcolemmal Na^+-Ca^{2+} exchanger. Biochim Biophys Acta. 1993; 1151:35–42. [PubMed: 8357818]

(21). Krishnamurthy H, Piscitelli CL, Gouaux E. Unlocking the molecular secrets of sodium-coupled transporters. Nature. 2009; 459:347–355. [PubMed: 19458710]

(22). Cordes FS, Bright JN, Sansom MS. Proline-induced distortions of transmembrane helices. J Mol Biol. 2002; 323:951–960. [PubMed: 12417206]

(23). Sansom, J. N. B. a. M. S. P. The Flexing/Twirling Helix: Exploring the Flexibility about Molecular Hinges Formed by Proline and Glycine Motifs in Transmembrane Helices. J. Phys. Chem. B. 2003; 107:627–636.

(24). Liu W, Eilers M, Patel AB, Smith SO. Helix packing moments reveal diversity and conservation in membrane protein structure. J Mol Biol. 2004; 337:713–729. [PubMed: 15019789]

(25). Henzler-Wildman K, Kern D. Dynamic personalities of proteins. Nature. 2007; 450:964–972. [PubMed: 18075575]

(26). Henzler-Wildman KA, Lei M, Thai V, Kerns SJ, Karplus M, Kern D. A hierarchy of timescales in protein dynamics is linked to enzyme catalysis. Nature. 2007; 450:913–916. [PubMed: 18026087]

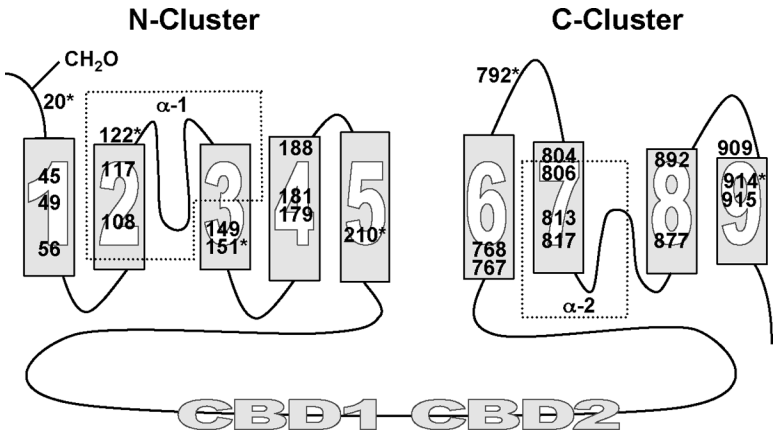

Fig. 1. Topological model of the cardiac Na^+/Ca^{2+} exchanger and location of amino acids studied in this work

Transmembrane segments are represented by *rectangles*, the α-repeat regions are surrounded by boxes and the location of the regulatory Ca^{2+}-binding domains are indicated by "CBD". The predicted locations of the residues mutated to cysteine are shown. Endogenous cysteines of the native exchanger that were reintroduced into the cysteineless NCX1 are indicated with asterisks.

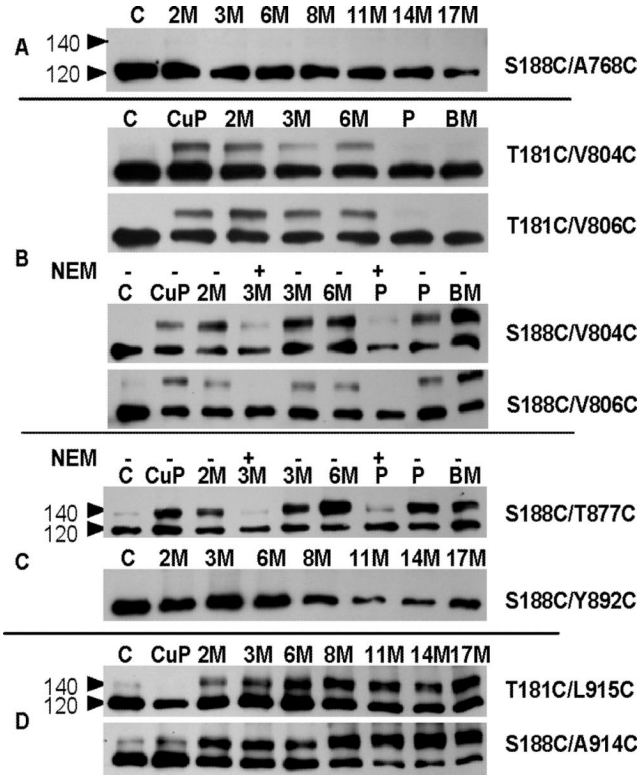

Fig. 2. Crosslinking between residues in TMS 4 and residues in the C-cluster of TMSs

(A) Crosslinking between TMSs 4 and 6. **(B)** Crosslinking between TMSs 4 and 7. **(C)** Crosslinking between TMSs 4 and 8. **(D)** Crosslinking between TMSs 4 and 9. High Five cells were transfected with the indicated double cysteine mutant cDNAs and 24 h later, intact cells were treated with crosslinkers as indicated in Experimental Procedures for 20 min at room temperature. Proteins were separated by SDS-PAGE under *non-reducing* conditions, transferred to nitrocellulose membranes, and then probed with an anti-exchanger antibody. The presence of a band at 140 kDa indicates crosslinking between the introduced cysteine residues. Some experiments show that preincubation with the membrane permeable reagent NEM blocks subsequent crosslinking. C = control, no crosslinkers added; CuP = CuPhe; P = *p*-PDM; BM = BM(PEG)2.

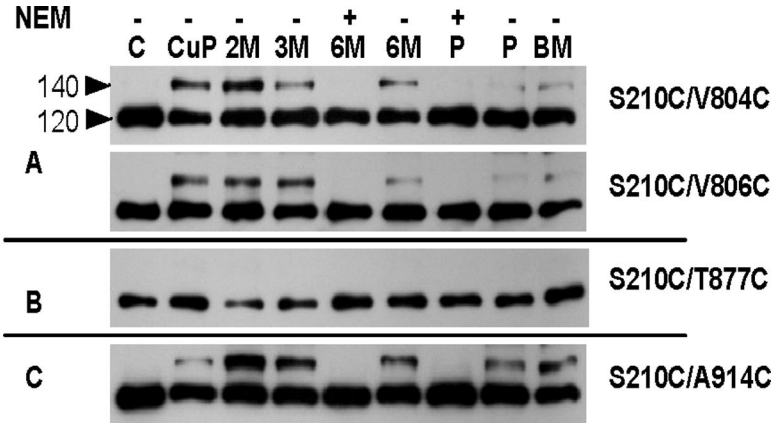

Fig. 3. Crosslinking between residues in TMS 5 with residues in the C-cluster of TMSs

(A) Crosslinking between TMSs 5 and 7. **(B)** Lack of crosslinking between TMSs 5 and 8. **(C)** Crosslinking between TMSs 5 and 9. Experiments were performed as described in Fig. 2.

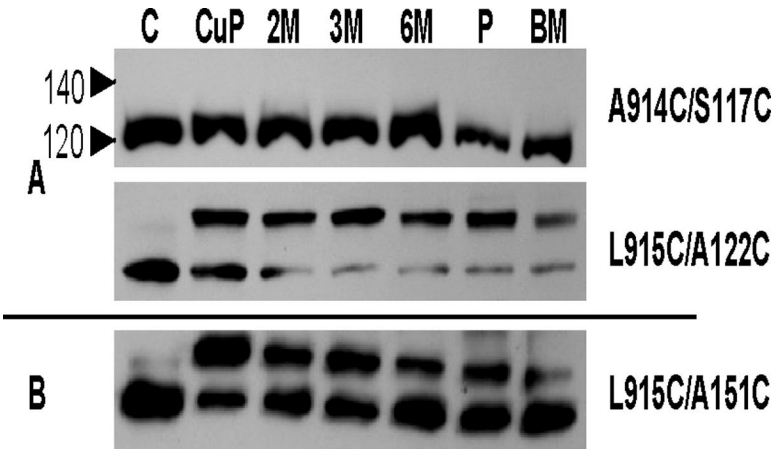

Fig. 4. Crosslinking between residues in TMS 9 and residues in the N-cluster of TMSs

(A) Crosslinking between TMSs 9 and 2. **(B)** Crosslinking between TMSs 9 and 3. Experiments were performed as described in Fig. 2.

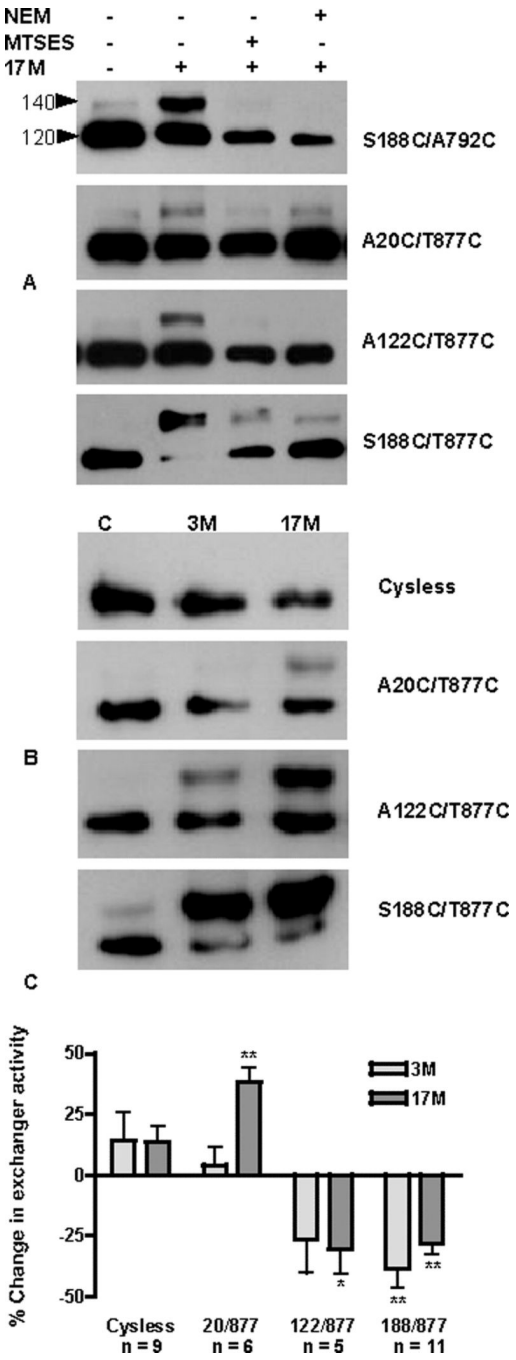

Fig. 5. Crosslinking between T877C, modeled to be at intracellular surface of TMS 8, with extracellular residues

(A) The indicated mutants were expressed in High Five cells, preincubated with MTSES or NEM, and then checked for crosslinking with 17M as described in Fig. 2. **(B)** Crude membrane vesicles from transfected insect High Five cells were prepared as described in `Experimental Procedures', treated with 50 μM of 3M or 17M for 30 min at room temperature and subjected to SDS-PAGE under non-reducing conditions and transferred to a nitrocellulose membrane for immunoblots. **(C)** Vesicular exchange activity of the mutants after treatment with 3M or 17M. Data are presented as means ± SD (T-test p * <0.05 or **<0.01, as indicated, compared to untreated vesicles; n = 5–11 as indicated).

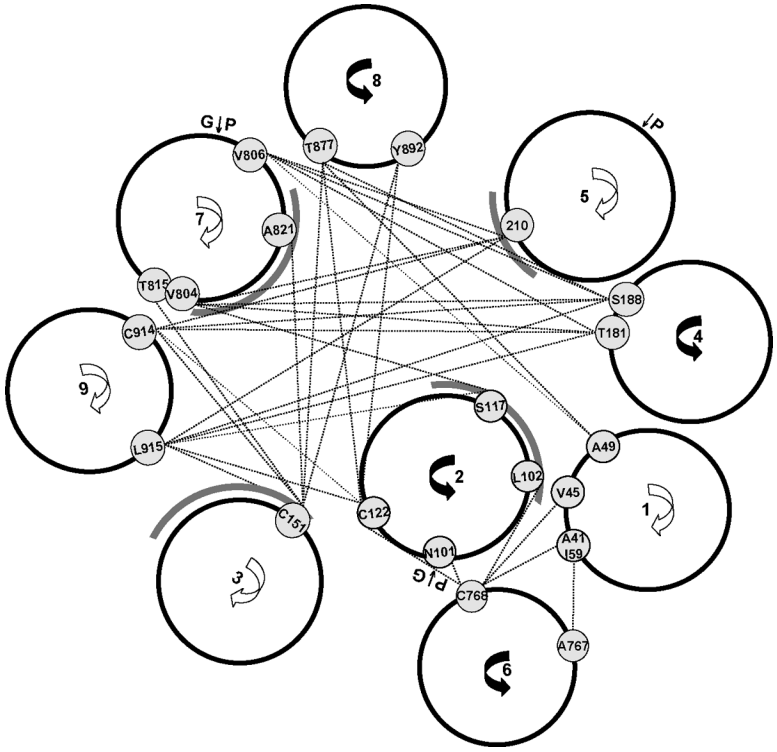

Fig. 6. Computer Generated model of NCX1 Helix packing

All crosslinking data (Table 1) from this and previous work (12,14) were combined to generate the model. Pairs of residues that demonstrated crosslinking are indicated with lines. The faces of TMSs that contain residues that have altered activity upon mutagenesis are indicated with grey arcs.

Biochemistry. Author manuscript; available in PMC 2011 October 5.

Table 1

Disulfide crosslinking of exchanger mutants

		N-Cluster																	
C-Cluster		TMS 1								TMS 2					TMS 3		TMS 4		TMS 5
		40	41	42	43	45	49	58	59	101	102	106	117	122	151	172	181	188	210
TMS 6	767		+*b*						+*b*									−	
	768		+*b*			+*b*	− *b*	− *a*	+*b*	+*b*	+*b*	− *a*		+*b*	− *a*	− *a*		−	− *a*
	788	− *b*	− *b*		− *a*								− *a*	− *a*				− *a*	
	789		− *b*	− *b*															
TMS 7	804				− *a*								+*a*	− *a*			+	+	+
	806					−	+										+	+	+
	815							− *a*				− *a*			+*a*	− *a*			− *a*
	819							− *a*				− *a*			+*a*	− *a*			− *a*
	821							− *a*				− *a*			+*a*	− *a*			− *a*
	822							− *a*				− *a*			− *a*	− *a*			− *a*
TMS 8	875							− *a*				− *a*			− *a*	− *a*			− *a*
	877					−	+							+	+			+	−
	892	− *b*	− *b*	− *b*	− *a*				− *b*				− *a*	+*a*	+			−	
TMS 9	907	− *b*	− *b*	− *b*					− *b*										
	909	− *b*	− *b*	− *b*	− *a*				− *b*				+*a,c*	− *a*				− *a*	
	912	− *b*	− *b*						− *b*										
	914												−	+	+		+	+	+
	915												+	+	+		+	+	+
	923	− *b*	− *b*	− *b*					− *b*										
	926							− *a*				− *a*			− *a*	− *a*			− *a*

All other data were collected in this work. −, no crosslinking observed; +, crosslinking observed; grey shading highlights data used to construct helix-packing model.

[a] data published in (1)

[b] data published in (2)

[c] inactive mutant, not included to define packing model